S-matrix parametrization as a way of locating quantum resonances and bound states: multichannel case

P. O. G. Ogunbade and S. A. Rakityansky

Department of Physics, University of Pretoria, Lynnwood Road, Pretoria 0002, South Africa

Abstract. A method is proposed for analytic continuation of the multi-channel *S*-matrix given at a finite number of discrete points on the real axis of the energy. Using its values at these points, it is possible to calculate the *S*-matrix at complex energies on any sheet of the Riemann surface within a wide band along the real axis. The method is based on the established analytic properties of the multi-channel Jost matrices and a rational (Padé-type) approximation of the *S*-matrix obtained at real collision energies. Numerical examples demonstrate the stability and accuracy of the proposed method.

Keywords: Jost matrices, quantum resonances, Padé approximation

INTRODUCTION

It is often necessary to identify the spectral points (i.e. bound and resonance states) and extract their energies and widths from experimental scattering data available over some energy range. For a single-channel problem, a method for solving such a problem was proposed in Ref. [1].

The main idea is based on the coincidence principle [2]: two analytic functions coinciding on a curve segment are identical everywhere in the complex plane. Therefore, if we find a good analytic approximation of the *S*-matrix on the real axis, we may expect that it is also valid at the nearby points of the complex plane (or Riemann surface). In particular, such an approximate *S*-matrix should have the same singularities, i.e. the spectral points, which thus can be located.

In Ref. [1], the given *S*-matrix values are fitted using a meromorphic function of the Padé type, which is a ratio of two polynomials. In this work, we extend the method to a multi-channel problem, where before using the Padé approximation, the threshold branching points are explicitly factorized in each element of the Jost matrix.

RATIONAL APPROXIMATION OF THE *S*-MATRIX

We assume that the complex-valued matrices[1] $\mathbf{S}_\ell(E)$ are known at discrete points within a finite energy segment $[E_{min}, E_{max}]$ along the real axis. These can be either the experimental points or the values obtained theoretically using some numerical procedure.

---

[1] In this paper, all the matrices are labeled using bold symbols.

Let us look for an approximate matrix $\widetilde{\mathbf{S}}_\ell(E)$ such that its difference from the given ("exact") values $\mathbf{S}_\ell(E)$ is minimal on the segment $[E_{\min}, E_{\max}]$. Keeping in mind the coincidence principle, we hope that the more accurately we approximate the S-matrix on the real axis, the less different will be the poles of $\widetilde{\mathbf{S}}_\ell(E)$ at complex energies from the corresponding poles of the "exact" $\mathbf{S}_\ell(E)$.

In this work, the functional form we chose for the approximate S-matrix is known in numerical analysis as the matrix Padé approximant of the order $[M,M]$ given by

$$\widetilde{\mathbf{S}}_\ell(E) = \mathbf{P}(E)[\mathbf{Q}(E)]^{-1} = \left[\sum_{m=0}^{M} \mathbf{p}_m E^m\right] \cdot \left[\sum_{m=0}^{M} \mathbf{q}_m E^m\right]^{-1} \tag{1}$$

where the $\mathbf{p}_m$ and $\mathbf{q}_m$ are some unknown matrices of fitting parameters.

The form of the Padé approximation that we use is different from the standard approach in the following. The standard matrix Padé approximant [3, 4] requires the function to have a Taylor series representation. Our method, however, uses only the values of the function at discrete points on the real axis. Similarly to the single-channel case, the order $[M,M]$ (equal orders of the "numerator" and "denominator") of the Padé approximant ensures that at high energies $\mathbf{S}_\ell(E) \to \mathbf{I}$ [5] where $\mathbf{I}$ is the identity matrix. The other difference is that we incorporate the correct low energy behaviour of the S-matrix into our fitting procedure which is discussed next.

Multi-Channel Jost matrices

Consider an N-channel problem with the threshold energies E_n^{th}, channel momenta

$$k_n = \sqrt{\frac{2\mu_n}{\hbar^2}(E - E_n^{\text{th}})}, \tag{2}$$

and channel angular momenta ℓ_n ($n = 1, 2, \ldots, N$). The multi-channel S-matrix can be written as the "ratio"

$$\mathbf{S}_\ell(E) = \mathbf{F}_\ell^{(\text{out})}(E) \cdot \left[\mathbf{F}_\ell^{(\text{in})}(E)\right]^{-1} \tag{3}$$

of the Jost matrices $\mathbf{F}_\ell^{(\text{in/out})}(E)$ which are the amplitudes of the incoming and outgoing spherical waves in the asymptotic behaviour

$$\mathbf{\Phi}_\ell(E,r) \xrightarrow[r\to\infty]{} \mathbf{H}^{(-)}{}_\ell(E,r)\mathbf{F}_\ell^{(\text{in})}(E) + \mathbf{H}^{(+)}{}_\ell(E,r)\mathbf{F}_\ell^{(\text{out})}(E) \tag{4}$$

of the fundamental matrix $\mathbf{\Phi}_\ell$ of regular solutions of the system of radial Schrödinger equations. Here the diagonal matrices

$$\mathbf{H}^{(\pm)} = \mathtt{diag}\{h_{\ell_1}^{(\pm)}(k_1 r), h_{\ell_2}^{(\pm)}(k_2 r), \ldots, h_{\ell_N}^{(\pm)}(k_N r)\} \tag{5}$$

are composed of the Riccati-Hankel functions. Looking for the fundamental matrix $\mathbf{\Phi}_\ell(E,r)$ in the form

$$\mathbf{\Phi}_\ell(E,r) = \mathbf{J}_\ell(E,r)\mathbf{A}(E,r) - \mathbf{N}_\ell(E,r)\mathbf{B}(E,r) \tag{6}$$

where $\mathbf{J}$ and $\mathbf{N}$ are diagonal matrices composed of the Riccati-Bessel and Riccati-Neumann functions,

$$\mathbf{J} = \mathtt{diag}\{j_{\ell_1}(k_1 r), j_{\ell_2}(k_2 r), \ldots, j_{\ell_N}(k_N r)\} \,, \tag{7}$$

$$\mathbf{N} = \mathtt{diag}\{n_{\ell_1}(k_1 r), n_{\ell_2}(k_2 r), \ldots, n_{\ell_N}(k_N r)\} \,, \tag{8}$$

we obtain [6] (from the Schrödinger equation) the following system of differential equations for the new unknown matrices $\mathbf{A}(E,r)$ and $\mathbf{B}(E,r)$

$$\begin{cases} \partial_r \mathbf{A} = -\mathbf{K}^{-1} \mathbf{N} \mathbf{V} (\mathbf{J} \mathbf{A} - \mathbf{N} \mathbf{B}) \\ \partial_r \mathbf{B} = -\mathbf{K}^{-1} \mathbf{J} \mathbf{V} (\mathbf{J} \mathbf{A} - \mathbf{N} \mathbf{B}) \end{cases} \tag{9}$$

with the boundary conditions

$$\mathbf{A} \xrightarrow[r \to 0]{} \mathbf{I}, \qquad \mathbf{B} \xrightarrow[r \to 0]{} \mathbf{0} \tag{10}$$

where the diagonal momentum matrix $\mathbf{K}$ is given by

$$\mathbf{K} = \mathtt{diag}\{k_1, k_2, \ldots, k_N\} \,. \tag{11}$$

The matrices $\mathbf{A}$ and $\mathbf{B}$ are related to the Jost matrices via their asymptotic values

$$\mathbf{F}^{(\mathrm{in})}(E) = \lim_{r \to \infty} \frac{1}{2} [\mathbf{A}(E,r) - i\mathbf{B}(E,r)] \,, \tag{12}$$

$$\mathbf{F}^{(\mathrm{out})}(E) = \lim_{r \to \infty} \frac{1}{2} [\mathbf{A}(E,r) + i\mathbf{B}(E,r)] \,. \tag{13}$$

At any finite r, the expressions on the right hand sides of Eqs. (12, 13) give the corresponding Jost matrices for the potential truncated at the point r (similarly to the variable-phase approach).

Since Eqs. (9) involve the channel momenta, their solutions and therefore the Jost matrices (being functions of E) depend on the energy via all k_n. This makes them multivalued functions of the energy. Indeed, for any chosen E, we have two possibilities for choosing the sign in front of the square root

$$k_n = \pm\sqrt{\frac{2\mu_n}{\hbar^2}(E - E_n^{\mathrm{th}})}, \tag{14}$$

for each channel momentum. Therefore the Jost matrices have 2^N different values at each point E. In other words, they are defined on the Riemann surface consisting of 2^N interconnecting sheets. The branching points are at the threshold energies $E_n^{(\mathrm{th})}$.

The complications caused by the multivaluedness of the matrices $\mathbf{A}$ and $\mathbf{B}$ can be avoided in the following way. Let us consider the well known power series expansions

of the Riccati-Bessel and Riccati-Neumann functions [7],

$$
\begin{aligned}
j_\ell(kr) &= k^{\ell+1} \sum_{n=0}^{\infty} k^{2n} \left[\frac{(-1)^n \sqrt{\pi}}{\Gamma(\ell + \frac{3}{2} + n)n!} \left(\frac{r}{2}\right)^{2n+\ell+1} \right] \\
&= k^{\ell+1} \sum_{n=0}^{\infty} k^{2n} \gamma_{\ell n}(r) = k^{\ell+1} \widetilde{j}_\ell(E,r)
\end{aligned}
\tag{15}
$$

$$
\begin{aligned}
n_\ell(kr) &= k^{-\ell} \sum_{n=0}^{\infty} k^{2n} \left[\frac{(-1)^{n+\ell+1} \sqrt{\pi}}{\Gamma(-\ell + \frac{1}{2} + n)n!} \left(\frac{r}{2}\right)^{2n-\ell} \right] \\
&= k^{-\ell} \sum_{n=0}^{\infty} k^{2n} \eta_{\ell n}(r) = k^{-\ell} \widetilde{n}_\ell(E,r).
\end{aligned}
\tag{16}
$$

where the odd powers of the momenta are factorized, namely, the factors $k^{\ell+1}$ and $k^{-\ell}$. Such a factorization for the matrices $\mathbf{J}$ and $\mathbf{N}$ gives

$$
\begin{aligned}
\mathbf{J} &= \mathtt{diag}\left\{ k_1^{\ell_1+1}, k_2^{\ell_2+1}, \ldots, k_N^{\ell_N+1} \right\} \widetilde{\mathbf{J}} \\
\mathbf{N} &= \mathtt{diag}\left\{ k_1^{-\ell_1}, k_2^{-\ell_2}, \ldots, k_N^{-\ell_N} \right\} \widetilde{\mathbf{N}}
\end{aligned}
\tag{17}
$$

After the factorization, the remaining series involve only the even powers of k and thus the functions $\widetilde{\mathbf{J}}$ and $\widetilde{\mathbf{N}}$ are single-valued functions of the energy.

Substituting the factorized expressions for $\mathbf{J}$ and $\mathbf{N}$ into Eqs. (9) and looking for matrices $\mathbf{A}$ and $\mathbf{B}$ in the factorized form

$$
A_{mn} = \frac{k_n^{\ell_n+1}}{k_m^{\ell_m+1}} \widetilde{A}_{mn}, \qquad B_{mn} = k_m^{\ell_m} k_n^{\ell_n+1} \widetilde{B}_{mn}
\tag{18}
$$

we see that all the factors composed of the odd powers of the momenta cancel out and the matrices $\widetilde{\mathbf{A}}$ and $\widetilde{\mathbf{B}}$ satisfy the following modified coupled differential equations

$$
\begin{cases}
\partial_r \widetilde{\mathbf{A}} = -\widetilde{\mathbf{N}} \mathbf{V} \left(\widetilde{\mathbf{J}}\widetilde{\mathbf{A}} - \widetilde{\mathbf{N}}\widetilde{\mathbf{B}} \right) \\
\partial_r \widetilde{\mathbf{B}} = -\widetilde{\mathbf{J}} \mathbf{V} \left(\widetilde{\mathbf{J}}\widetilde{\mathbf{A}} - \widetilde{\mathbf{N}}\widetilde{\mathbf{B}} \right),
\end{cases}
\tag{19}
$$

with the boundary conditions

$$
\widetilde{\mathbf{A}} \xrightarrow[r \to 0]{} \mathbf{I}, \qquad \widetilde{\mathbf{B}} \xrightarrow[r \to 0]{} \mathbf{0}.
\tag{20}
$$

It is seen that the differential equations (19) do not involve any channel momenta k_n. This means that $\widetilde{\mathbf{A}}(E,r)$ and $\widetilde{\mathbf{B}}(E,r)$ are single-valued matrix functions of the energy E.

Therefore, the Jost matrices have the following structure

$$
F_{mn}^{(\mathrm{in})}(E) = \frac{1}{2} \left[\frac{k_n^{\ell_n+1}}{k_m^{\ell_m+1}} \widetilde{A}_{mn}(E) - i k_m^{\ell_m} k_n^{\ell_n+1} \widetilde{B}_{mn}(E) \right],
\tag{21}
$$

$$
F_{mn}^{(\mathrm{out})}(E) = \frac{1}{2} \left[\frac{k_n^{\ell_n+1}}{k_m^{\ell_m+1}} \widetilde{A}_{mn}(E) + i k_m^{\ell_m} k_n^{\ell_n+1} \widetilde{B}_{mn}(E) \right],
\tag{22}
$$

They are multi-valued functions and the branching points are determined by the factors

$$\frac{k_n^{\ell_n+1}}{k_m^{\ell_m+1}} \qquad \text{and} \qquad k_m^{\ell_m} k_n^{\ell_n+1}. \qquad (23)$$

Apparently, the "in" and "out" Jost matrices are related to each other on different sheets of the Riemann surface, namely,

$$F_{mn}^{(\text{out})}(E, k_1, k_2, \dots) = (-1)^{\ell_m+\ell_n} F_{mn}^{(\text{in})}(E, -k_1, -k_2, \dots), \qquad (24)$$

and thus

$$\mathbf{S}(E) = \mathbf{F}^{(\text{out})}(E) \left[\mathbf{F}^{(\text{in})}(E) \right]^{-1}$$
$$= (-1)^{\ell_n+\ell_m} \mathbf{F}^{(\text{in})}(E, -k_1, -k_2, \dots, k_N) \left[\mathbf{F}^{(\text{in})}(E, k_1, k_2, \dots, k_N) \right]^{-1}. \qquad (25)$$

It is important to point out that according to equation (24) not all the parameters in equation (1) are independent. This symmetry property (24) enables us to reduce the number of fitting parameters in half and also improves the quality of the approximation since the correct structure of the *S*-matrix, given by equation (25), is taken into account.

FITTING PARAMETERS

To begin with, we expand the matrices $\widetilde{\mathbf{A}}$ and $\widetilde{\mathbf{B}}$ in power series of E, since they are single-valued matrix functions (see the statement following equation (19)), we have

$$\widetilde{\mathbf{A}}(E) \approx \sum_{\mu=0}^{M} \boldsymbol{\alpha}^{(\mu)} E^{\mu}, \qquad \widetilde{\mathbf{B}}(E) \approx \sum_{\mu=0}^{M} \boldsymbol{\beta}^{(\mu)} E^{\mu}. \qquad (26)$$

It is clear from equation (26) that we have to determine $2(M+1)$ unknown matrices $\boldsymbol{\alpha}^{(\mu)}$ and $\boldsymbol{\beta}^{(\mu)}$ ($\mu = 0, 1, 2, \dots, M$).

Let us assume that there are $2(M+1)$ *S*-matrix data given on the interval $[E_{\min}, E_{\max}]$ of the real energy axis. The method of calculating the parameters $\boldsymbol{\alpha}^{(\mu)}$ and $\boldsymbol{\beta}^{(\mu)}$ is as follows. We multiply equation (25) by $\mathbf{F}^{(\text{in})}$ from the right and re-write it as

$$\mathbf{F}^{(\text{out})}(E_i, k_1, k_2, \dots) = \mathbf{S}(E_i) \mathbf{F}^{(\text{in})}(E_i, k_1, k_2, \dots), \qquad i = 1, 2, \dots, 2(M+1). \qquad (27)$$

Substituting equations (21) and (22), into equation (27), after some matrix algebra and rearrangements, we find that this is a linear system of equations for $\alpha_{mn}^{(\mu)}$ and $\beta_{mn}^{(\mu)}$, given by

$$\sum_{\mu=0}^{M} \left[\frac{k_n^{\ell_n+1}}{k_m^{\ell_m+1}} \left(S_{mm}(E_i) - 1 \right) \alpha_{mn}^{(\mu)} - \imath k_m^{\ell_m} k_n^{\ell_n+1} \left(S_{mm}(E_i) + 1 \right) \beta_{mn}^{(\mu)} \right.$$
$$\left. + \sum_{\substack{j=1 \\ j \neq m}}^{N} S_{mj}(E_i) \left(\frac{k_n^{\ell_n+1}}{k_j^{\ell_j+1}} \alpha_{jn}^{(\mu)} - \imath k_j^{\ell_j} k_n^{\ell_n+1} \beta_{jn}^{(\mu)} \right) \right] E_i^{\mu} = 0 \qquad (28)$$

where $m, n = 1, 2, \ldots, N$; $i = 1, 2, \ldots, 2(M+1)$. Similarly to the single channel case, we can simplify the last equation by including into it the correct behaviour of the S-matrix at zero collision energy [5]:

$$S_{mm}(E) \xrightarrow[k_m \to 0]{} 1 + O(k_m^q), \quad q \geq \ell + 1$$

$$S_{mn}(E) \xrightarrow[k_m \to 0]{} O(k_m^q), \quad m \neq n, \ q \geq \ell + 1/2,$$

we thus obtain

$$\sum_{\mu=1}^{M} \left[\frac{k_n^{\ell_n+1}}{k_m^{\ell_m+1}} \left(S_{mm}(E_i) - 1 \right) \alpha_{mn}^{(\mu)} - \iota k_m^{\ell_m} k_n^{\ell_n+1} \left(S_{mm}(E_i) + 1 \right) \beta_{mn}^{(\mu)} \right. $$
$$\left. + \sum_{\substack{j=1 \\ j \neq m}}^{N} S_{mj}(E_i) \left(\frac{k_n^{\ell_n+1}}{k_j^{\ell_j+1}} \alpha_{jn}^{(\mu)} - \iota k_j^{\ell_j} k_n^{\ell_n+1} \beta_{jn}^{(\mu)} \right) \right] E_i^{\mu} = \delta_{mn} - S_{mn}(E_i) \tag{29}$$

where $i = 1, 2, \ldots, 2M$, $\alpha_{mn}^{(0)} = \delta_{mn}$, $\beta_{mn}^{(0)} = 0$ and δ_{mn} is the Kronecker delta ($m, n = 1, 2, \ldots, N$).

Having obtained the parameters $\boldsymbol{\alpha}^{(\mu)}$ and $\boldsymbol{\beta}^{(\mu)}$, we can search the spectral points at complex energies as the roots of the determinant of the matrix function $\mathbf{F}^{\text{in}}$ (i.e. the poles of the S-matrix (25))

$$\det \left[\mathbf{F}^{\text{in}}(E) \right] = 0, \tag{30}$$

where the matrix elements of $\mathbf{F}^{\text{in}}$ are given by

$$F_{mn}^{\text{in}}(E) = \frac{1}{2} \sum_{\mu=0}^{M} \left[\frac{k_n^{\ell_n+1}}{k_m^{\ell_m+1}} \alpha_{mn}^{(\mu)} - \iota k_m^{\ell_m} k_n^{\ell_n+1} \beta_{mn}^{(\mu)} \right] E^{\mu}. \tag{31}$$

NUMERICAL EXAMPLES

As an illustration of how the suggested method works, we performed numerical calculations for two two-channel problems, namely: exactly solvable model of coupled square-wells [8, 5] and Noro-Taylor model potential [9]. The test conducted here is mainly for $\ell_1 = \ell_2 = 0$, although any channel angular momenta can be handled by our method. In both cases N fitting points (input energies) were chosen and uniformly distributed on the interval $E_{\min} \leqslant E \leqslant E_{\max}$ on the real axis i.e.

$$E_n = E_{\min} + \frac{E_{\max} - E_{\min}}{N - 1} (n - 1), \qquad n = 1, 2, \ldots, N \tag{32}$$

The exact values of the $\mathbf{S}$-matrix at the fitting points were calculated using a very accurate method, which is based on a combination of the complex rotation and a direct calculation of the Jost matrix function as described in [6]. The locations of the exact spectral points were obtained by the same method.

The first of the testing potentials is an exactly solvable model problem coupled by square-well potentials [5], shown in Figure 1. The units in this model are chosen in such a way that $\mu_1 = \mu_2 = \hbar c = 1$. The channel threshold energies are $E_1^{th} = 0.0$ and $E_2^{th} = 2.0$, while the interaction potential have the forms

$$\mathbf{V}(r) = \begin{cases} \mathbf{U} & \text{for } 0 \leq r \leq 1 \\ \mathbf{0} & \text{otherwise} \end{cases}$$

$$\mathbf{U} = -\begin{pmatrix} 2.0 & 0.5\lambda \\ 0.5\lambda & 2.0 \end{pmatrix}, \qquad \lambda = 0 \text{ or } 1. \tag{33}$$
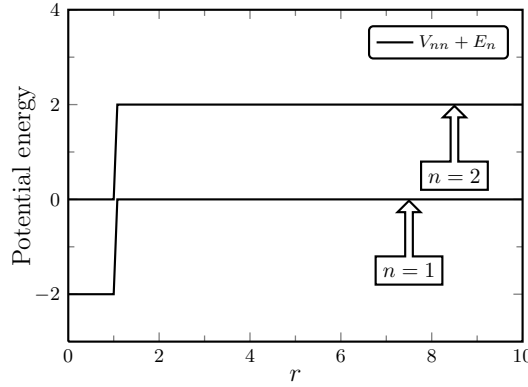
FIGURE 1. Square-well diagonal channel potentials (33). The potentials are shifted by the threshold energies E_n.

Although, this model problem is known to have exact analytical solution [5], numerical calculations as discussed above were employed to generate the **S**-matrix and the spectral points. In the absence of coupling between the channels (i.e. $\lambda = 0$), the diagonal potentials each generates a single bound state. These bound states are located at $E_1 = -0.2035507418$ and $E_2 = 1.7964592582$. When the coupling is switched on ($\lambda = 1$) only the lower bound state survived with shifted energy: $E_1 = -0.2430965098$. The bound state of the upper potential $V_{22}(r) + E_2^{th}$ can now decay into the continuum of the lower potential $V_{11}(r) + E_1^{th}$, thus turning into a resonance. The corresponding pole of the **S**-matrix is located on an unphysical sheet of the complex energy Riemann surface at $E_2 = 1.8315168862 - i0.0290733625$.

To give some indication of the accuracy of the rational approximation Table 1 shows the positions of the bound states and resonance for a series of approximants ranging from $N = 2$ to $N = 10$, with $E_{\min} = 1$ and $E_{\max} = 8$.

The second test case is shown in Figure 2. It supports bound states, resonances and sub–threshold resonances [1]. In the units such that $\mu_1 = \mu_2 = \hbar = 1$, the potential has the form

$$\mathbf{V}(r) = \begin{pmatrix} -1.0 & -7.5 \\ -7.5 & 7.5 \end{pmatrix} r^2 e^{-r} \tag{34}$$

The thresholds energies are $E_1^{th} = 0$ and $E_2^{th} = 0.1$. The exact **S**-matrix corresponding

TABLE 1. Convergence of the poles of the approximate $\tilde{\mathbf{S}}(E)$ found for the potential (33) using N fitting points evenly distributed over the interval $1 \leqslant E \leqslant 8$. All values are given in the arbitrary units such that $\mu_1 = \mu_2 = \hbar = 1$. λ is the switching parameter.

		$\lambda = 0$		$\lambda = 1$	
ID	N	Re E	Im E	Re E	Im E
E_1	2	0.9346579288	-0.2046585820	0.9696684253	-0.1914384518
	5	-0.2020229243	-1.24×10^{-12}	-0.2422637171	-1.1×10^{-14}
	7	-0.2035497226	-1.46×10^{-11}	-0.2430955910	-2.2×10^{-11}
	10	-0.2035506639	1.54×10^{-10}	-0.2430964602	-8.4×10^{-10}
	Exact	-0.2035507418		-0.2430965098	
E_2	2	1.2144390251	6.71×10^{-16}	1.2539964140	-0.0861903892
	5	1.7964492680	3.03×10^{-15}	1.8315169134	-0.0290733682
	7	1.7964492581	-2.12×10^{-14}	1.8315168861	-0.0290733625
	10	1.7964492581	4.54×10^{-13}	1.8315168861	-0.0290733625
	Exact	1.7964492582		1.8315168862	-0.0290733625
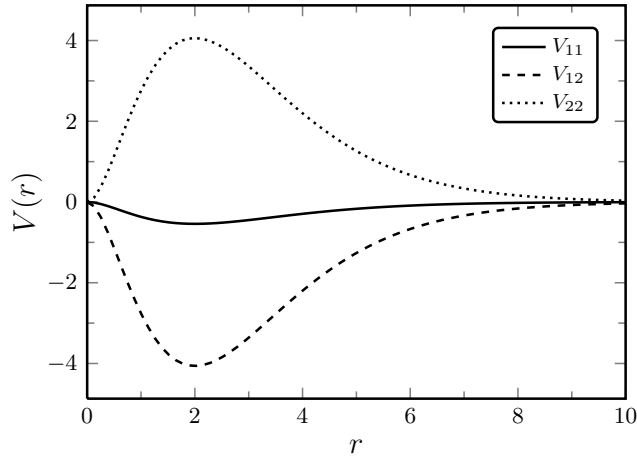
FIGURE 2. The Noro–Taylor potential [9] model given in Equation (34).

to this potential has an infinite number of poles forming a string that goes down the E-plane to infinity. The exact locations of the first six of the S-wave resonance states are given in Table 2. We compared the S-wave resonance poles obtained using $N = 30$ of the approximated $\tilde{\mathbf{S}}$-matrix where $E_{\min} = 1$ and $E_{\max} = 10$ with the exact locations. Figure 3 shows the accuracy of the proposed method. Just as it was expected, the most significant poles i.e. those that are close to the real axis and the fitting segment were reproduced correctly. The fitting points on the real E-axis are indicated by vertical bars. In Table 3, the exact and approximate $\tilde{\mathbf{S}}$-matrix poles are compared for the first five resonances generated by the potential (34).

TABLE 2. The *S*-wave resonance poles, $\hbar^2 k_n^2 = 2\mu_n(E - E_n^{\text{th}})$, of the exact **S**-matrix obtained for the Noro–Taylor potential (34). They were obtained using the rigorous Jost-function method described in [6]. All the values are given in the arbitrary units such that $\mu_1 = \mu_2 = \hbar = 1$.

no.	Re E	Im E	Re k_1	Im k_1	Re k_2	Im k_2
1	4.768197	−0.000710	3.088105	−0.000230	3.055551	−0.000232
2	7.241200	−0.755956	3.810742	−0.198375	3.784482	−0.199752
3	8.171217	−3.254166	4.119051	−0.790028	4.095577	−0.794556
4	8.440526	−6.281492	4.354528	−1.442520	4.333805	−1.449417
5	8.072643	−9.572815	4.538158	−2.109405	4.520027	−2.117867
6	7.123813	−13.012669	4.686027	−2.776909	4.670234	−2.786299

TABLE 3. Comparison of the first five resonance points for the potential (34) for $\ell = 0$. They (Exact) were obtained using the rigorous Jost-matrix function method [6] and the Padé approximation (Approx.) with the number of fitting points $N = 30$ evenly distributed over the interval $1 \leqslant E \leqslant 10$ (the units are such that $\mu_1 = \mu_2 = \hbar = 1$.

ℓ	no.		Re E	Im E
0	1	Exact	4.768197	−0.000710
		Approx.	4.768197	−0.000710
	2	Exact	7.241200	−0.755956
		Approx.	7.241200	−0.755956
	3	Exact	8.171217	−3.254166
		Approx.	8.171199	−3.254177
	4	Exact	8.440526	−6.281492
		Approx.	8.431643	−6.261440
	5	Exact	8.072643	−9.572815
		Approx.	8.846481	−9.353923

CONCLUSION

In this paper, we propose a method by which one can obtain an approximate analytic expression for the *S*-matrix valid at complex energies when the *S*-matrix is given at a set of points on the real axis of the energy. Such an expression can be used, for example, to locate the poles of the multichannel *S*-matrix which may correspond to bound and resonant states of a system. Compared to the previous description [1] we have here extended it from single-channel case to multichannel problems. The only requirements for this method is a table of the *S*-matrix data along the real *E*-axis for which rational-fraction analytical continuation to complex energy plane has been proven to converge rapidly.

The numerical examples show that the proposed method is stable and accurate. With just a few fitting points, it reproduces the bound states and the most significant reso-
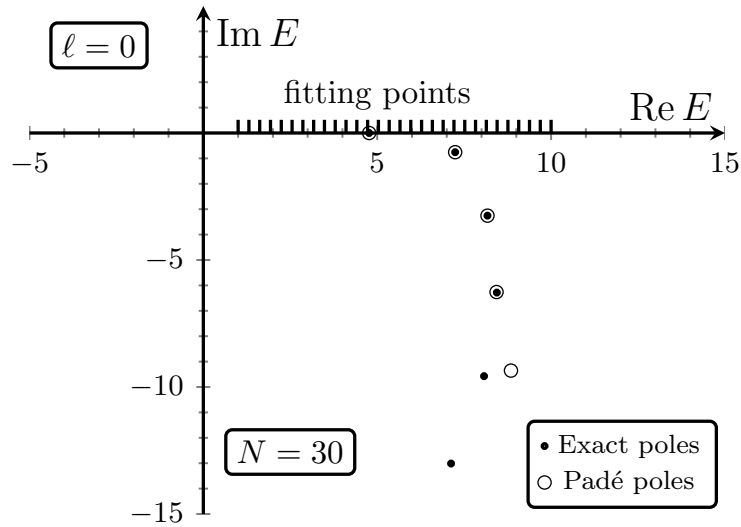
FIGURE 3. The exact positions of the *S*-wave resonance poles (dots) on the complex energy plane for the potential (34), and the corresponding poles of the Padé approximation (open circles). The corresponding fitting points on the $\mathrm{Re}\,E$-axis are indicated by vertical bars.

nances to the accuracy that is sufficient for any practical purposes.

ACKNOWLEDGMENTS

REFERENCES

1. S. A. Rakityanski, S. A. Sofianos, and N. Elander, *J. Phys. A: Math. Theor.* **40**, 14857–14869 (2007).
2. R. P. Boas, *Invitation to Complex Analysis*, Random House, New York, 1987.
3. W. H. Press, S. A. Teukolsky, W. T. Vetterling, and B. P. Flannery, *Numerical Recipes in FORTRAN*, Cambridge University Press, Cambridge, 1992.
4. G. A. Baker, and J. L. Gammel, editors, *The Padé Approximant in Theoretical Physics*, Academic, New York, 1970.
5. R. G. Newton, *Scattering Theory of Waves and Particles*, Springer-Verlag, New York, 1982, 2nd edn.
6. S. A. Rakityanski, and N. Elander, *Int. J. Quantum Chem.* **106**, 1105 (2006).
7. M. Abramowitz, and I. A. Stegun, *Handbook of Mathematical Functions*, National Bureau of Standards, Washington, D.C., 1964.
8. S. Han, and W. P. Reinhardt, *J. Phys. B: At. Mol. Opt. Phys.* **28**, 3347–3367 (1995).
9. T. Noro, and H. S. Taylor, *J. Phys. B: Atom. Molec. Phys.* **13**, L377 (1980).